MOLECULAR PHYSICS, 1999, VOL. 97, NO. 1/2, 35–42

Interpreting vibrationally resolved spectra of molecular dications (doubly positively charged molecules): HCl^{2+}

FREDERICK R. BENNETT[1], ANDREW D. J. CRITCHLEY[2], GEORGE C. KING[3], ROBERT J. LEROY[4] and IAIN R. MCNAB[2]*

[1] Comachem, PO Box 1542, Nhulunbuy, NT 0881, Australia
[2] Department of Physics, University of Newcastle upon Tyne, Newcastle upon Tyne NE1 7RU, UK
[3] Department of Physics and Astronomy, University of Manchester, Manchester M13 9PL, UK
[4] University of Waterloo, Ontario, N2L 3G1, Canada

(*Received 27 November 1998; accepted 23 December 1998*)

Vibrationally resolved spectra of HCl^{2+} appear to show five vibrational levels for the $X\,^3\Sigma^-$ ground electronic state, whereas calculations of vibrational levels supported by *ab initio* potential energy curves have been able to locate only three vibrational levels below the barrier; this discrepancy is resolved by considering vibrational states that the potential function supports in the continuum above the barrier maximum. A low resolution spectrum produced from first principles is compared with a spectrum obtained with threshold photoelectrons in coincidence (TPEsCO) spectroscopy, with agreement sufficient to suggest that care must be taken in the inversion of vibrational spectroscopic data for molecular dications to avoid generating potential functions that are too strongly bound.

1. Introduction

The structure of molecular dications (doubly positively charged molecules) is the focus of increasing attention [1, 2] from both theoreticians who calculate potential energy surfaces [3, 4], and from experimentalists who measure low [5–7] and high [8–16] resolution spectra. Dications are of interest as candidates for energy storage [17], as possible XUV laser media [18], and as species important in the ionosphere and the interstellar medium [19]. The potential energy curves for many diatomic dications are unusual, having a minimum, a maximum and an asymptote below both. There has been discussion about the nature of these potential curves; the current consensus is that such curves do not represent an avoided crossing but are better considered as the sum of a Coulomb repulsion and molecular bonding forces [20]. The potential energy curve for the ground electronic state of HCl^{2+} is typical, and is shown as the upper state in figure 1. The barrier in the potential energy curve supports vibration–rotation states (shown as solid lines), but they lie above the dissociation limit, and therefore are quasi-bound. The lifetimes of such levels may vary dramatically, and in the potential well shown the lowest level has a calculated tunnelling lifetime of 6.5 h whereas the highest classically bound level has a calculated tunnelling lifetime of 1.1×10^{-13} s.

Historically, the properties of even diatomic dications have proved notoriously difficult to calculate [20, 21]; comparatively recent calculations by respected theoreticians have proved to be significantly in error. The principal reason for this appears to be that the properties of the dication are critically dependent upon the barrier height and width, and due to their unusual nature require very different types of basis set from neutral molecules; such bases are difficult to generate [22].

High resolution spectra of molecular dications have proved difficult to obtain; rotationally resolved spectra of only three molecular dications have been published, N_2^{2+} [8–14], NO^{2+} [15] and DCl^{2+} [16] (a high resolution spectrum of CO^{2+} may have been discovered [23]). The best guides to the search for high resolution spectra are the low resolution spectra that have been published. It is therefore of interest to consider how best to interpret the low resolution spectra of molecular dications.

Two vibrationally resolved spectra of HCl^{2+} have been published; Auger electron spectra of both HCl^{2+} and DCl^{2+} were obtained [5], while McConkey *et al.* [6] measured a threshold photoelectrons in coincidence (TPEsCO) spectrum of HCl^{2+} (a combination of the

* Author for correspondence. e-mail: iain.McNab@ncl.ac.uk

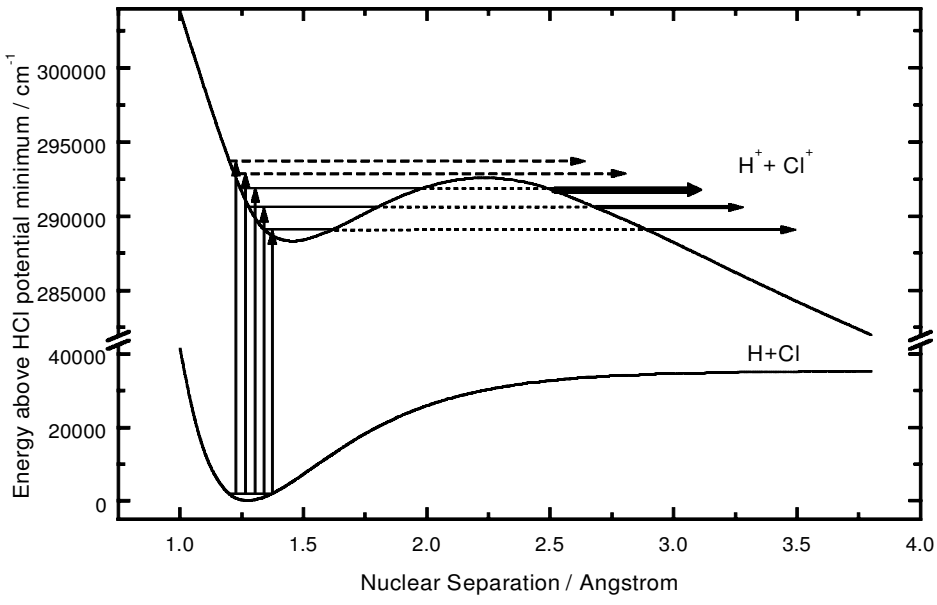

Figure 1. Single-photon double-ionization; HCl $\rightarrow$ HCl^{2+}. Included on the dication potential are the orbiting resonances it supports.

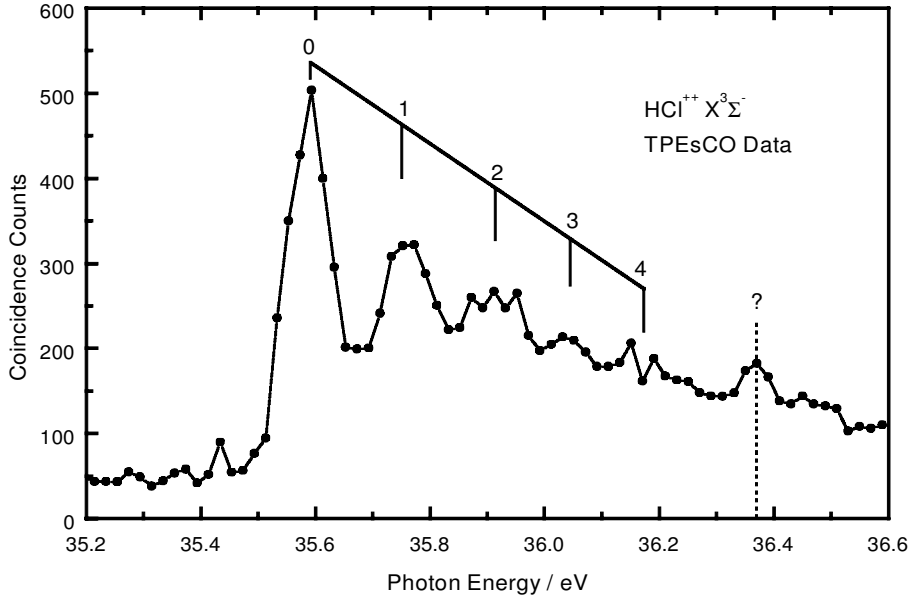

Figure 2. TPEsCO results for the $X\,^3\Sigma^-$ state of HCl^{2+} (75.77% H^{35}Cl^{2+}, 24.23% H^{37}Cl^{2+}). Threshold electron coincidence counts as a function of energy [6].

two isotopes H^{35}Cl^{2+} and H^{37}Cl^{2+} in their natural abundance), which recorded the coincidence counts from single-photon double-ionization, the process illustrated in figure 1. In both experiments measurements of the vibrational structure arising from transitions from HCl to HCl^{2+} showed five vibrational levels of the ground electronic ($X\,^3\Sigma^-$) state of HCl^{2+}. We reproduce the relevant portion of the TPEsCO work in figure 2.

The spectrum shows four clear peaks, numbered $v = 0$-3. In addition, a fifth peak ($v = 4$) was assigned which may be genuine. This assignment is uncertain in the light of the poor signal to noise ratio of the results. Nonetheless, these results were interpreted as five quasi-bound levels supported below the barrier of the HCl^{2+} potential. The Auger data were obtained at similar resolution. In the case of the Auger spectrum, the authors used the observed vibrational progression to construct a plausible potential energy curve for HCl^{2+} by summing a Coulomb repulsion (c/R) potential and a Morse potential in such a manner as to give a barrier height which trapped the five vibrational levels that they observed.

Three high quality first-principles calculations of the ground electronic state of HCl^{2+} have been published. Olsson and Larsson [24] studied the $X\,^3\Sigma^-$, $a\,^1\Delta$ and low lying (dissociative) $^3\Pi$ states and Banichevich *et al.* [25] made more accurate calculations of the potential energy functions of the electronic states correlating to the five

lowest dissociation asymptotes of HCl^{2+}. The most accurate calculations for the ground state so far published are by Bennett and McNab [4]. All the calculations found that only three vibrational levels could be supported within the ground state potential well. It is difficult to draw conclusions about convergence between the calculations because of the different methods applied to the problem. Bennett and McNab investigated the convergence of their potential with respect to the radial and angular dimensions of the one-particle basis set and concluded that the three vibrational levels supported below the barrier maximum were an upper bound because increases to the basis set size further decreased the energy difference between the minimum and maximum of the potential.

Recent rotationally resolved experimental measurements by Abusen *et al.* [16] on the infrared spectrum of $D^{35}Cl^{2+}$ are in good agreement with a theoretical spectrum calculated with the potential energy function of Bennett and McNab [4]. The vibrational band origin is within $20\,cm^{-1}$ of the experimental band origin, and the calculated and measured rotational structure are in excellent agreement. The discrepancy between (a) the good agreement of high resolution spectra and theory and (b) the apparently poor agreement of low resolution spectra and the same theory is the motivation for the present study. In addition to the $HCl^{2+}(DCl^{2+})$ discrepancies, there has been some conjecture over resonances located at energies above calculated barrier heights of the $^3\Pi_g$ state of N_2^{2+} [13, 26].

Classically, vibrational motion can occur only within a potential, but quantum mechanically there is a probability for a particle to be reflected by a barrier, even if it has sufficient energy (classically) to travel over it. Such continuum vibrations have large probabilities only at certain resonant energies. These energies are determined by the shape of the potential above which they occur; the vibrational structure is a continuation of the normal vibrational progression within a potential well into the continuum above it.

The potential barriers in diatomic molecular dications support resonances in the continuum. We have calculated the resonance structure that is supported below and above the potential barrier of Bennett and McNab's potential function for HCl^{2+}. We performed the calculations with the program BCONT [27, 28] which normally is used to produce absorption coefficients for electronic transitions within a molecule, but in this case is used to calculate the absorption coefficients for single-photon double-ionization. To justify using the program in this way, the Born–Oppenheimer approximation, which states that the electrons expelled in the ionization process have no influence on the final state wavefunction, was applied. For an Auger spectrum this approximation should be excellent—for the TPEsCO measurements, which claim to be made at 'threshold', the photoelectrons should have approximately zero energy, and it is less obvious that the approximation is good. However, our calculations appear to be in good agreement with the TPEsCO observations and this provides a post-facto justification. We find two short-lived (wide), large amplitude resonances are supported by the HCl^{2+} potential above the barrier maximum. Both of these continuum resonances have sufficient amplitude to be seen in low resolution experiments, but such large widths that they are unlikely to be observed in high resolution experiments.

2. Quasibound levels of dications as continuum resonances

In calculations of vibration–rotation levels supported by diatomic dication potential energy functions it has been the almost universal practice to solve the radial Schrödinger equation for the quasibound states below the maximum of the potential barrier. However, all such levels are in fact resonances within the continuum above the dissociation asymptote, and a more satisfactory procedure is to calculate all vibration–rotation levels as resonances in a continuum. The solution of the bound state problem alone will always omit continuum resonances if they are present. Some methods of solving bound state problems by using artificial scattering channels [29] do not suffer from this problem, but the calculations are computationally intensive.

Bound-continuum photodissociation calculations are used to investigate the resonance structure supported by the dication potentials at energies both below and above the barrier maximum. At most energies below the maximum, the eigenfunctions in the well region have very small amplitudes [30]. However, over narrow energy intervals centred approximately at the eigenvalues the potential would have if its asymptote was at the barrier maximum, the wavefunction amplitude in the well region becomes very large, which reflects the presence of orbiting resonances or quasibound levels. In a bound-continuum photodissociation calculation, the region of non-negligible wavefunction overlap usually includes this well region, so the absorption cross-section will show a narrow intensity maximum due to the local maximum amplitude inside the potential energy barrier.

Resonances above a barrier maximum do not just occur in molecular dications, but anywhere where there is such a barrier maximum, such as above a rotational barrier (see e.g., [31]) or above a barrier resulting from an avoided crossing. The continuum resonances for 'normal' potential energy curves, are observable only at high angular momenta, and therefore have seldom been observed in normal spectroscopic experi-

Table 1. Energies and widths calculated with LEVEL for the rotationless vibrational levels supported below the potential maximum of four isotopes of HCl^{2+}. The potential maximum lies at 4313.16 cm^{-1} above the local minimum.

Isotope	v	Energy above potential minimum/cm^{-1}	Γ/cm^{-1}
$H^{35}Cl^{2+}$	0	827.09	2.73×10^{-10}
	1	2333.48	6.17×10^{-5}
	2	3601.43	0.803
$H^{37}Cl^{2+}$	0	826.48	2.66×10^{-10}
	1	2331.89	6.02×10^{-5}
	2	3599.34	0.788
$D^{35}Cl^{2+}$	0	598.51	2.24×10^{-16}
	1	1721.27	1.29×10^{-10}
	2	2736.15	8.82×10^{-6}
	3	3617.59	8.16×10^{-2}
	4	4295.95	44.7
$D^{37}Cl^{2+}$	0	597.65	2.08×10^{-16}
	1	1718.91	1.20×10^{-10}
	2	2732.65	8.27×10^{-6}
	3	3613.48	7.73×10^{-2}
	4	4292.61	43.5

ments. Two methods are used in this study to investigate the resonant structure of the HCl dication: a bound state type approach which locates the level using an effective outer boundary condition and calculates the width semiclassically, and a direct simulation of the bound to continuum photodissociation cross-sections. There are many other techniques for the determination of resonance energies and positions, notably the collisional time delay method [32] and semiclassical methods based upon this [33].

3. Quasibound levels and resonance structures in HCl^{2+}

We have calculated the energies and widths of resonances both above and below the barrier maximum with the bound state program LEVEL [34] and the photodissociation program BCONT [27, 28] . LEVEL determines the discrete eigenvalues and eigenfunctions of the radial Schrödinger equation with a subroutine based on the work of Cooley, Cashion, and Zare [35–37]. The Numerov method (see, e.g., [38]) is used to integrate the Schrödinger equation numerically over a user-specified range. An Airy function boundary condition is employed to find resonances [32], and the semiclassical time delay method of Connor and Smith [33] is used to determine the widths.

The energies and widths obtained with LEVEL are shown in table 1. LEVEL cannot calculate the resonances above the barrier; to do so requires a continuum calculation such as that provided by BCONT. However, it is far less computationally intensive to solve the radial Schrödinger equation using LEVEL, so this is still the best procedure for the levels below the barrier maximum in most cases.

Table 2. Comparison of LEVEL and BCONT data for the quasibound levels of $H^{35}Cl^{2+}$. Γ_L/Γ_B provides a comparison of the linewidths.

v	J	Peak energy/cm^{-1} [a]	BCONT Γ_B/cm^{-1}	LEVEL Γ_L/cm^{-1}	Γ_L/Γ_B
0	0	287 626.76	3.00×10^{-10}	2.73×10^{-10}	0.910
	4	287 574.82	5.60×10^{-10}	5.47×10^{-10}	0.977
	9	287 391.51	6.10×10^{-9}	5.80×10^{-9}	0.951
1	0	289 134.07	6.25×10^{-5}	6.17×10^{-5}	0.987
	4	289 070.09	1.12×10^{-4}	1.08×10^{-4}	0.964
	9	288 843.86	7.60×10^{-4}	7.34×10^{-4}	0.966
2	0	290 402.67	0.83	0.80	0.964
	4	290 322.55	1.25	1.20	0.960
	9	290 036.10	4.76	4.64	0.975
3	0–9	291 721.05	362		
4	0–9	291 960.10	4785		

[a] Transition energy calculated with BCONT.

A full photodissociation calculation of the resonance structure of transitions from HCl to HCl^{2+} was made with the program BCONT. The program evaluates the radial matrix elements between the eigenfunctions representing the discrete initial-state levels and the energy normalized final-state continuum wavefunctions, as mediated by a transition moment function $M(R)$. In the absence of a first principles calculation of the transition moment function, we assumed a constant function (of unity). We considered only transitions from the ground vibrational state of HCl (the only one significantly populated at the temperatures (~300 K) used in the experiments). At room temperature 99% of the rotational population resides in $J < 10$, so we have considered only $J < 10$ in our simulations of HCl^{2+}. Usually it is found that no rotational excitation occurs in direct ionization processes; the rotational populations which must be considered therefore are those of the HCl ground vibrational state. The selection rules governing photodissociation are $\Delta J = 0, \pm 1$, but we have not considered this explicitly because the radial matrix elements change slowly with ΔJ, so a Q branch approximation, $\Delta J = 0$ only, is sufficient [28]. Table 2 summarizes some of the results obtained with BCONT and compares the widths with the corresponding widths from the LEVEL calculations. The figures show remarkable agreement between the linewidths predicted by the two methods. The $v = 0$ resonance widths could not be found directly with BCONT, since the minimum energy mesh of the

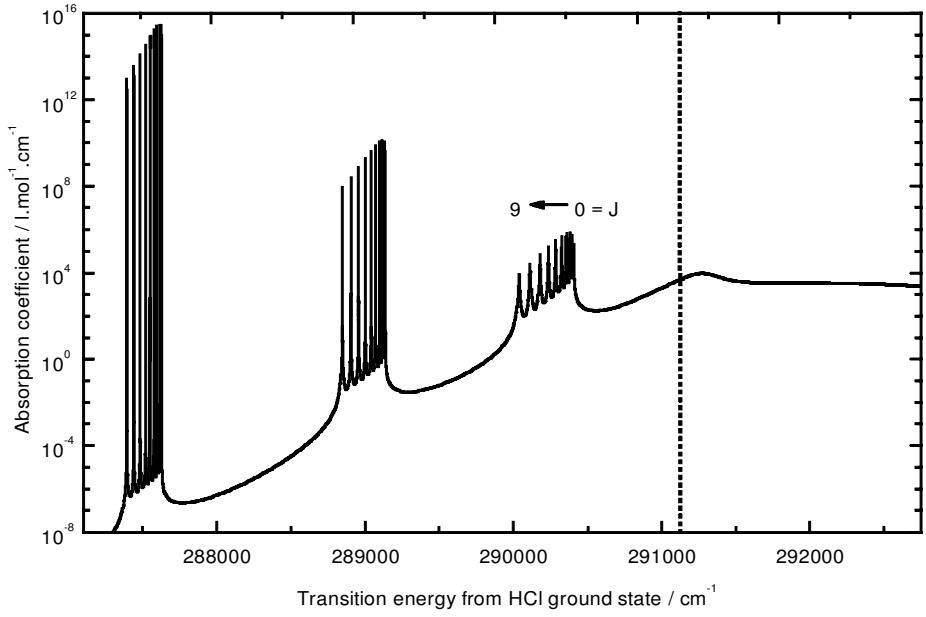

Figure 3. Resonance structure of the $X\,^3\Sigma^-$ state of HCl^{2+}: a plot of absorption coefficient (or photodissociation cross-section) against transition energy from the ground state $(v, J = 0, 0)$ of HCl.

program is $10^{-10}\,cm^{-1}$. The data for each peak was fitted to a Lorentzian lineshape, the widths of which are given in table 2.

Figure 3 shows the resonant structure calculated for HCl^{2+}, which is an addition of separate calculations suitably weighted for $H^{35}Cl^{2+}$ and $H^{37}Cl^{2+}$. The data shown were calculated with an energy mesh of $0.04\,cm^{-1}$. This is sufficient to define the $v = 2$ peaks and the continuum structure, but the maxima of the lower energy peaks had to be found separately with a finer mesh appropriate to the linewidth in question. In figure 3, the peak values found in this way replace the value corresponding to the mesh point nearest to the peak. The finest mesh available to us was $10^{-10}\,cm^{-1}$ whereas the narrowest resonance has a width of $3 \times 10^{-10}\,cm^{-1}$, so in the case of the narrowest resonances the peaks were found by fitting a Lorentzian lineshape to the calculated cross-section points. The absorption coefficients for $H^{37}Cl^{2+}$ have been scaled down by a factor of 0.319, which corresponds to the ratio of the natural abundance of the two isotopes. The plot is logarithmic to emphasize the states which exist above the barrier (the barrier maximum position is indicated by a dashed line). The continuum resonances can be seen more clearly later in figures 4 and 5. The amplitudes of the resonances decrease dramatically above the barrier, but the resonances have substantial width, and their integrated intensities are large.

4. Simulated spectra

In order to compare our calculated resonance positions and widths with the experimentally observed low resolution spectra we have convoluted the resonance structure with a lineshape function. We have attempted to reproduce the TPEsCO measurements, and have convoluted the data with a Gaussian function of 115 meV full width at half maximum to match the widths of the TPEsCO spectrum. The convolution process is described by the integral

$$I(f) = i(f) * g(f) = \int_{-\infty}^{\infty} i(f - v)g(v)\,dv.$$

In this case $i(f)$ represents the BCONT data, $g(f)$ is a normalized Gaussian lineshape function and $I(f)$ is the simulated observed intensity. The calculation involved a simple numerical integration of the data in figure 3 and its multiplication with a Gaussian function integrated over the same frequency range on a grid of points separated by $0.04\,cm^{-1}$. The integration was started two linewidths below the minimum frequency and finished two linewidths above the maximum frequency of the BCONT data. Before integration the $v = 0$ and 1 peak values had to be modified, since they have widths many orders of magnitude smaller than the grid spacing used. For the case where $i(f)$ is very much narrower than $g(f)$ the convolution is approximated very accurately by

$$I(f) = g(f - f_0) \int_{-\infty}^{\infty} i(f - f_0)\,df,$$

where f_0 is the centre frequency of $i(f)$. We used this approximation to modify the narrow $i(f)$ functions onto the grid used for the calculation. The areas beneath the narrow peaks were calculated with a fine frequency mesh ($10^{-10}\,cm^{-1}$) and used to obtain effective peaks which produced equivalent areas on the $0.04\,cm^{-1}$ mesh in the numerical integration. More sophisticated

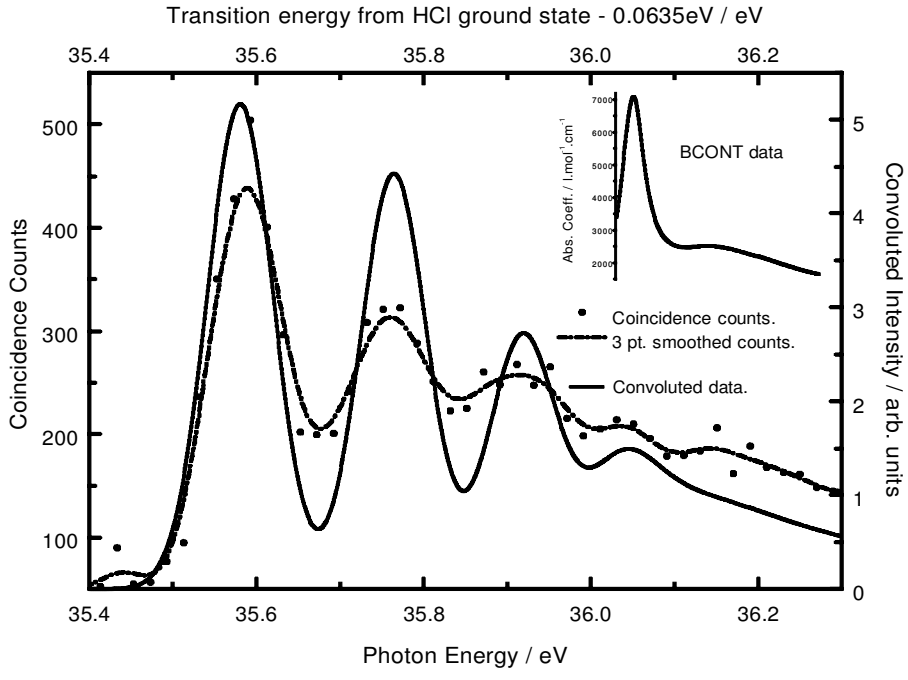

Figure 4. Comparison of the TPEsCO spectrum with the BCONT data convoluted with a 115 meV Gaussian function. Inset: plot of the continuum reonance data, which reveal the second continuum resonance lost in the convoluted spectrum.

methods of convolution, such as fast Fourier transforms (see, e.g., [39]) are not suited to the integration of resonances orders of magnitude smaller than the convoluting function.

The theoretical calculations and the experimental spectrum are compared in figure 4. As can be seen, the relative spacings of the peaks are reproduced closely by our calculations (although for comparison the convoluted spectrum in the figure has been shifted down in energy by 0.0635 eV). The three quasibound levels and a further resonance can be distinguished clearly, whereas the second resonance above the potential barrier is not evident after convolution. However, as shown in the inset of figure 4, the predicted position of the second resonance above the barrier matches that of the fifth peak of the TPEsCO spectrum. The relative intensities of the peaks are not reproduced well, since these depend directly on the transition moment function for the photo double-ionization, and we have not calculated this function (nor, to our knowledge, has one been reported in the literature). The assumption of a constant transition moment function is believed to be a major cause of the discrepancies in intensity. The other obvious cause of discrepancies are inadequacies in the potential energy functions. Ideally we would wish to adjust the HCl^{2+} function iteratively to create agreement with the experimental data but this is not worthwhile in the absence of a suitable transition moment. The ground state of HCl was approximated to a Morse potential with the required molecular constants; the results are not very sensitive to the HCl function used, as the wavefunction for $v = 0$ is almost harmonic, but if a transition moment function were available an accurate ground state potential would be used.

The calculations have been repeated for DCl^{2+} using the same potential energy function. Here we have included $J < 13$ to take account of over 98% of the rotational population. The structure in the continuum is compared with that obtained for HCl^{2+} in figure 5. In DCl^{2+} two resonances were found by the photodissociation calculation; one is centred below the barrier and is also found in the bound state calculation. The difference between the above barrier resonances for the same potential illustrates the significance of the reduced mass in the calculation—for a given potential the reduced mass determines the energy above the barrier at which the resonances appear, and this strongly influences their width and intensity.

In DCl^{2+}, the resonance centred in the continuum is unlikely to be observed in a low resolution experiment, since the convolution of the BCONT data with the same Gaussian function as the HCl^{2+} data (shown in figure 6) obscures all trace of it. The predicted spectrum has the same number of resonances as the Auger spectrum of DCl^{2+} [5]; also their relative positions are in agreement within the experimental error quoted. However, the use of a suitable transition moment function $M(R)$ might alter the amplitude, as we believe will be the case for the second continuum resonance in HCl^{2+}. Clearly, continuum resonances are more likely to be observed the closer they occur to the barrier maximum.

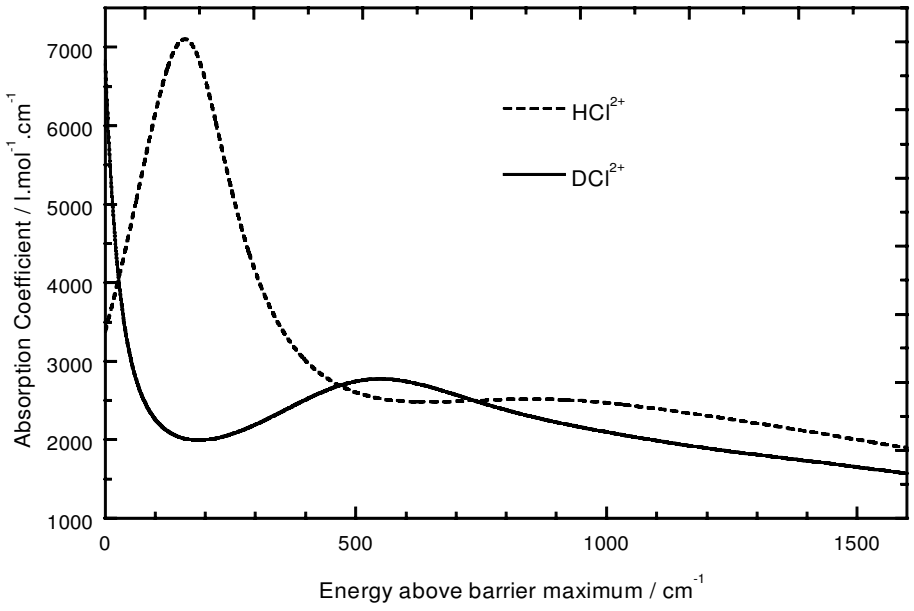

Figure 5. Continuum resonance structures of HCl^{2+} and DCl^{2+}.

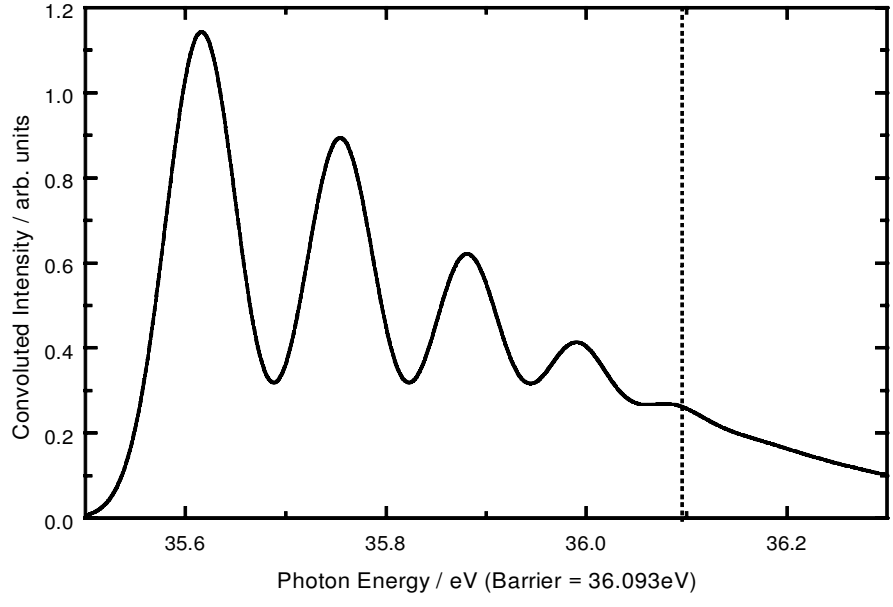

Figure 6. Predicted TPEsCO spectrum of DCl^{2+}. The potential maximum is indicated by the dotted line (= 36.093eV).

5. Conclusion

We are now in a position to reconcile completely the previous discrepancy between measured and calculated vibrational structure in HCl^{2+}. It is evident that in the case of HCl^{2+} any interpretation or inversion of low resolution vibrational data for diatomic dications must consider continuum resonances, although our study of DCl^{2+} has shown that the continuum resonances need not always be evident at low resolution. This result can be applied generally to all molecular dications; whether the continuum resonance structure is intense will depend on the potential and reduced mass in each case, and the energy of the resonance peaks relative to the barrier maximum. Resonance states are well known in molecular physics and often are observed in scattering experiments. Observation of resonance states by spectroscopic methods is not usual because their linewidths can be too great for detection. The intrinsically low resolution spectroscopic techniques which have been applied to the study of molecular dications have frequency widths which are comparable with the width of scattering states, and are ideally suited to their detection.

The low resolution spectrum calculated from the Bennett and McNab potential shows that two of the electron coincidence peaks from the TPEsCO spectrum of the $X\,^3\Sigma^-$ state of HCl^{2+} are continuum resonances, and

that the original interpretation was in error. This has serious implications for the analysis of spectra of this kind, as potential wells derived by inversion of experimental data may be too deep if the possibility of resonances above a potential barrier is not considered. In particular, in the normal 'forward' inversion (an iterative procedure where a spectrum is calculated for a trial potential energy function, and is used to modify the function for a better fit), the calculation of the spectrum must use scattering programs such as BCONT if the forward calculation is to be complete. In each case the details of the potential and the reduced mass used will determine the significance (or otherwise) of continuum resonances.

I.McN. is grateful to Professor J. M. Hutson and Dr J. F. McCann for suggesting a study of resonant structure. We are grateful to EPSRC and the Research Committee of the University of Newcastle upon Tyne for their support of our experimental work and to EPSRC for a studentship to A.D.J.C. We thank Professor A. S. Dickinson for useful discussions.

References

[1] Price, S. D., 1997, *J. chem. Soc. Faraday Trans.*, **93,** 2451.
[2] Mathur, D., 1993, *Phys. Rep.*, **225,** 193.
[3] Larsson, M., 1993, *Comments at. molec. Phys.*, **29,** 39.
[4] Bennett, F. R., and McNab, I. R., 1996, *Chem. Phys. Lett.*, **251,** 405.
[5] Svensson, S., Karlsson, L., Baltzer, P., Keane, M. P., and Wannberg, B., 1989, *Phys. Rev.* A, **40,** 4369; Karlsson, L., Blatzer, P., Svensson, S., and Wannberg, B., 1988, *Phys. Rev. Lett.*, **60,** 2473.
[6] McConkey, A. G., Dawber, G., Avaldi, L., Macdonald, M. A., King, G. C., and Hall, R. I., 1994, *J. Phys.* B, **27,** 271.
[7] Hochlaf, M., Hall, R. I., Penent, F., Eland, J. H. D., and Lablanquie, P., 1998, *Chem. Phys.*, **234,** 249.
[8] Carroll, P. K., 1958, *Can. J. Phys.*, **36,** 1585.
[9] Martin, P. A., Bennett, F. R., and Maier, J. P., 1994, *J. chem. Phys.*, **100,** 4766.
[10] Cossart, D., Launay, F., Robbe, J. M., and Gandara, G., 1985, *J. molec. Spectrosc.*, **113,** 142; Cossart, D., and Launay, F., 1985, *J. molec. Spectrosc.*, **113,** 159.
[11] Cosby, P. C., Möller, R., and Helm, H., 1983, *Phys. Rev.* A, **28,** 766.
[12] Masters, T. E., and Sarre, P. J., 1990, *J. chem. Soc. Faraday Trans.*, **86,** 2005.
[13] Szaflarski, D. M., Mullin, A. S., Yokoyama, K., Ashfold, M. N. R., and Lineberger, W. C., 1991, *J. phys. Chem.*, **95,** 2122 ; Mullin, A. S., Szaflarski, D. M., Yokoyama, K., Gerber, G., and Lineberger, W. C., 1992, *J. chem. Phys.*, **96,** 3636.
[14] Larsson, M., Sundstrom, G., Brostrom, L., and Mannervik, S., 1992, *J. chem. Phys.*, **97,** 1750; Sundsrtom, G., Carlson, M., Larsson, M., and Brostrom, L., 1994, *Chem. Phys. Lett.*, **218,** 17.
[15] Cossart, D., Bonneau, M., and Robbe, J. M., 1987, *J. molec. Spectrosc.*, **125,** 413.
[16] Abusen, R. A., Bennett, F. R., McNab, I. R., Sharp, D. N., Shiell, R. C., and Woodward, C. A., 1998, *J. chem. Phys.*, **108,** 1761.
[17] Nicolaides, C. A., 1989, *Chem. Phys. Lett.*, **161,** 547.
[18] Lesech, C., 1995, *Phys. Rev.* A, **51,** R2668.
[19] Prasad, S. S., and Furman, D. R., 1975, *J. Geophys. Res.*, **80,** 1360.
[20] Bennett, F. R., 1995, *Chem. Phys.*, **190,** 53 and references therein.
[21] Hurley, A. C., 1962, *J. molec. Spectrosc.*, **9,** 18.
[22] Wetmore, R. W., LeRoy, R. J., and Boyd, R. K., 1984, *J. phys. Chem.*, **88,** 6318.
[23] Cossart, D., and Cossart-magos, C., 1996, *Chem. Phys. Lett.*, **250,** 129.
[24] Olsson, B. J., and Larsson, M., 1987, *J. Phys.* B, **20,** L137.
[25] Banichevich, A., Peyerimhoff, S. D., Vanhemert, M. C., and Fournier, P. G., 1988, *Chem. Phys.*, **121,** 351.
[26] Senekowitsch, J., Oneil, S., Knowles, P., and Werner, H.-J., 1991, *J. phys. Chem.*, **95,** 2125.
[27] LeRoy, R. J., 1993, *University of Waterloo Chemical Physics Research Report*, CP-329R[3].
[28] LeRoy, R. J., 1989, *Comput. Phys. Commun.*, **52,** 383.
[29] Moss, R. E., 1993, *Molec. Phys.*, **80,** 1541.
[30] Mott, N. F., and Massey, H. S. W., 1965, *The Theory of Atomic Collisions* (3rd Edn Clarendon Press, Oxford) p. 63.
[31] Recamier, J., and Berrondo, M., 1998, *Revista Mexicana De Fisica*, **44,** 353.
[32] LeRoy, R. J., and Liu, W-K., 1978, *J. chem. Phys.* **69,** 3622.
[33] Connor, J. N. L., and Smith, A. D., 1981, *Molec. Phys.*, **43,** 397.
[34] LeRoy, R. J., 1996, *University of Waterloo Chemical Physics Research Report*, CP-555R.
[35] Cooley, J. W., 1961, *Math. Computation*, **15,** 363.
[36] Cashion, J. K., 1963, *J. chem. Phys.*, **39,** 1872.
[37] Zare, R. N., 1964, *J. chem. Phys.*, **40,** 1934.
[38] Murrell, J. N., and Bosanac, S. D., 1989, *Introduction to the Theory of Atomic and Molecular Collisions* (London: Wiley) appendix 4.
[39] Press, W. H., Flannery, B. P., Teukolsky, S. A., and Vetterling, W. T., 1986, *Numerical Recipes* (Cambridge University Press) p. 407.